Specific Ion Adsorption and Short-Range Interactions at the Air Aqueous Solution Interface

Viswanath Padmanabhan,* Jean Daillant,† and Luc Belloni
Laboratoire Interdisciplinaire sur l'Organisation Nanométrique et Supramoléculaire, SCM, bât. 125, CEA Saclay, F-91191 Gif-sur-Yvette Cedex, France

Serge Mora
UMR 5587 CNRS, Université Montpellier II, place Eugène Bataillon, F-34095 Montpellier Cedex 5, France

Michel Alba
Direction des Sciences de la Matière, CEA Saclay, F-91191 Gif-sur-Yvette Cedex, France

Oleg Konovalov
ESRF, 6 rue Jules Horowitz, B.P. 220, 38043 Grenoble Cedex, France
(Received 14 April 2007; published 24 August 2007)

We have investigated the surface composition of alkali-halide aqueous solutions using grazing incidence x-ray fluorescence. Using mixtures of salts as a means to enhance the short-range effects, small differences in concentration over a few angstrom could be resolved, with, for example I^- or $Br^- > Cl^-$. In order to explain our data, we need to include an effective potential accounting for the short-range (Å) solvent mediated couplings, responsible for specific effects together with dispersion forces. This attractive potential (few k_BT for halides) leads to concentration profiles which are in good agreement with recent numerical simulations.

DOI: 10.1103/PhysRevLett.99.086105 PACS numbers: 68.03.Cd, 61.10.Kw, 61.20.−p

There is a broad range of phenomena in biology, environmental, and physical sciences where ions of the same valency like Cl^- and Br^- have a dramatically different effect [1,2]. Since the seminal work of Hofmeister on protein stability in 1888 [3], such ''ion specific'' effects have been illustrated by many examples ranging from enzymatic activity [4] and amyloidosis [5] to humics stability [6] and halide heterogeneous chemistry in the atmosphere [7,8]. Ion specific effects generally follow direct or reverse order of the so-called Hofmeister series, which for anions is $SCN^- > ClO_4^- \approx I^- > Br^- > Cl^- > F^-$. For example, the surface tension and the surface potential of aqueous solutions (decreased by HCl and increased by NaCl) follow the series in reverse order [9].

In many of these examples interfacial effects appear to play a key role. However, there is presently no first-principles theory or general agreement on the mechanisms involved even for the apparently simple case of surface tension and surface potential at the air solution interface. Contrary to acids, inorganic salts and bases are found to increase the surface tension of pure water [9] which, based on Gibbs equation implies depletion. The original description of the surface tension of dilute (Debye-Hückel) electrolytes by Onsager and Samaras [10] took into account the repulsive image force experienced by any ion at the surface and predicted an increase in the surface tension [$d\gamma/dc \sim$ 1.2 (mN/m)/(mol/L)], smaller than generally observed. Since then, different ideas have been used for refining the theory and introducing ion specificity. The simplest phenomenological approach consists in including an ion-free layer [11], but ion hydration [12] and solvation [13] have also been incorporated in modified Poisson-Boltzmann equations. In 1997, Ninham and Yaminsky suggested that dispersion forces should play an important role and would introduce specificity [14]. Further extension on this idea was carried out using hypernetted chain (HNC) integral equation approximation at the primitive model level of description (ionic spheres immersed in a continuous dielectric solvent). This proved to be extremely successful in describing the osmotic coefficients in the bulk [15] but failed to predict the surface tension, pointing out the need for molecular level description of the solvent structure and the ions at the interface. Molecular dynamics simulation incorporating polarizable potentials have also been recently performed [16]. They predict a nonmonotonic distribution of ions with surface enhancement of anions and depletion of cations. The simplified picture emerging from the simulations is that the polarization of ion and solvent in the asymmetric surface environment can compensate for the partial loss of solvation in sufficiently large and polarizable ions, leading in the end to a surface affinity [17].

The presence of ions in the surface layer could be demonstrated by sum frequency generation [18,19] and second harmonic generation, but these techniques are limited by the knowledge of the interfacial depth. Electron spectroscopies have in principle the required depth (1 nm or less) and have been used on liquid jets [20] and deliquesced halide salts [21], where surface enhancement in the halide anion was observed. Finally, using x-ray reflectivity, no clear surface enhancement could be evidenced [22]. In order to overcome these limitations, we have performed grazing incidence x-ray fluorescence (GIXF)

experiments and we have determined the surface composition for different ionic solutions and mixtures at various concentrations directly on air-aqueous solution interface. Salts of high purity ($>99.9\%$–99.999%) purchased from Sigma-Aldrich were roasted overnight at 0.5 atm. Fresh stock solutions of 1 M concentration were prepared in Millipore® water ($>18\ \mathrm{M\Omega\,cm^{-1}}$, <10 ppb of organic contents) which is further diluted in steps of 0.1 M. Surface tension measurements for each concentration were carried out in a cleaned Teflon® dish using du-Nöuy ring method (Krüss tensiometer) at 25 °C. For GIXF experiments, nitrogen was bubbled before preparing the solution to reduce the content of dissolved oxygen in water, and for the photosensitive iodide salts, surface tension measurements were carried out in a light protected chamber. The x-ray measurements were carried out in helium filled enclosure to avoid interference of argon from the atmosphere. For hygroscopic salts, the concentration was determined using capillary ion analysis.

GIXF is a direct element specific, surface sensitive, and nondestructive technique in which the fluorescence from the ions (chemical sensitivity) is recorded as a function of the grazing angle of incidence (depth sensitivity). Below a critical angle for total external reflection, $\theta_c \sim 2.5$ mrad at 8026 eV, an evanescent wave propagates at the surface with a penetration depth $1/2\ \mathrm{Im}(k_z) \approx 4.6$ nm, where k_z is the normal component of the incident wave vector in the solution. Beyond the critical angle, the penetration depth increases to microns, providing a reference for bulk concentration. The experiments were performed at the ESRF beam line ID10B at energies of 8026 or 13 800 eV depending on the nature of the ion which needed to be excited. A full spectrum including fluorescence and elastic scattering from the bulk was recorded for each value of the grazing angle of incidence θ. K and L fluorescence lines in between Cl K_α (2622 eV) and Br K_α (11 924 eV) were recorded using a Röntec XFlash 1000 detector (Peltier cooled drift diode) giving access in these experiments to Cl^-, ClO_4^-, Br^-, I^-, K^+, and Cs^+.

After energy calibration, the fluorescence spectra were analyzed following Ref. [23], using a Gaussian peak for each line with an energy dependent width, a shelf, and a tail accounting for detector related phenomena. The fluorescence of each element was determined by linear fitting, whereas the parameters of the width, tail, and shelf fraction were determined using a nonlinear Levenberg-Marquardt algorithm. The result of the fitting procedure is the fluorescence intensity of each element i as a function of θ: $I_i \propto \int_0^\infty dz c_i(z) e^{-\alpha_i z}$. $c_i(z)$ is the concentration of ion i at depth z. $\alpha_i = 2\,\mathrm{Im}(k_z) + \mu_i$, with μ_i the linear absorption coefficient at the fluorescence energy of the ion i, which takes into account the reabsorption corrections. We then normalized the fluorescence intensities to the elastic scattering intensity I_{elas} in order to get rid of any dependency of the geometrical factor related to the experimental configuration. We finally note that the penetration length is larger than the expected characteristic lengths in the distribution and expand

$$\left(\frac{I_i}{I_{\mathrm{elas}}}\right)\Big/\left(\frac{I_i}{I_{\mathrm{elas}}}\right)_{\mathrm{bulk}} = 1 + \frac{\alpha_i \Gamma_i}{c_{i\infty}} - \frac{\alpha_i^2}{c_{i\infty}} \int_0^\infty dz z [c_i(z) - c_{i\infty}] + \cdots, \tag{1}$$

where $\Gamma_i = \int_0^\infty dz (c_i(z) - c_{i\infty})$ is the Gibbs surface excess, which is negative for depletion, with $c_{i\infty}$ the concentration of ion i in the bulk. Equation (1) provides direct access to the surface composition through Γ_i.

To demonstrate the validity of our approach, we have compared directly the fluorescence intensities from chloride (in HCl) and perchlorate (in $HClO_4$) anions where all the correction factors are similar since the fluorescence from chlorine only is considered. One can notice clearly in Fig. 1(a) that, below θ_c, the fluorescence from ClO_4^- is indeed more intense than that of Cl^-, agreeing well with the expectation that $HClO_4$ adsorbs more strongly at the

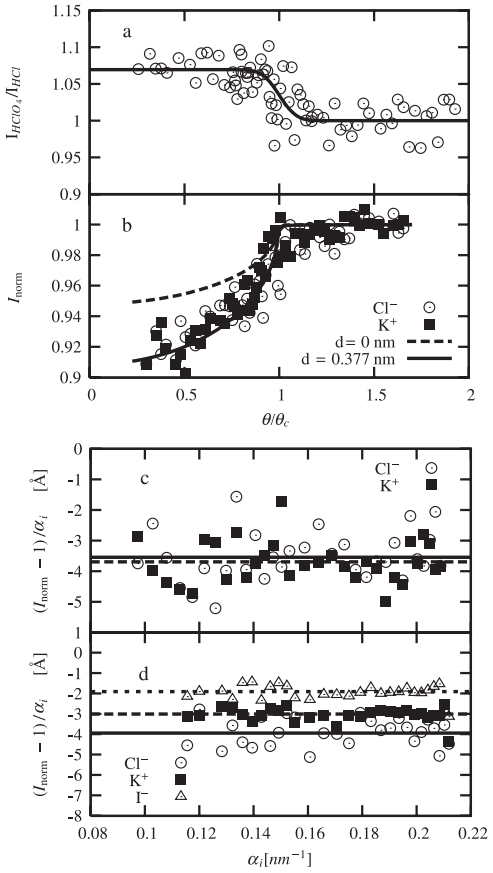

FIG. 1. (a) Ratio of the ClO_4^- (in 0.1 M $HClO_4$) and Cl^- (in 0.1 M HCl) fluorescence intensities. (b) Normalized K^+ and Cl^- intensities for 0.1 M KCl solution. Calculation considering the Coulombic image charge interactions only (dashed line) and an additional ion-free layer of 3.77 Å as expected from surface tension measurements (solid line) [11]. Here, I_{norm} refers to $[(I_{\mathrm{fluo}}/I_{\mathrm{elas}})/(I_{\mathrm{fluo}}/I_{\mathrm{elas}})_{\mathrm{bulk}}]$ for the ion i. $[I_{\mathrm{norm}} - 1]/\alpha_i$ as a function of α_i yielding $\Gamma_i/c_{i\infty}$ for 0.1 M KCl solution (c) and a mixture of 0.1 M KCl and 0.1 M KI solution (d).

interface than HCl. Quantitative analysis using Eq. (1) for 0.1 M potassium chloride (KCl) solution shows that the normalized fluorescence intensity is smaller below θ_c than above [Fig. 1(b)], implying a depletion of ions at the interface. Comparison to a model calculation shows that the depletion is stronger than what is predicted from image forces only [Fig. 1(b)]. Fitting the model of Ref. [11] against our data, a better agreement is obtained by incorporating an additional ion-free layer of 3.77 Å in good agreement with the surface tension data [11]. This value can be directly recovered using Eq. (1) by plotting $[(I_i/I_{\mathrm{elas}})/(I_i/I_{\mathrm{elas}})_{\mathrm{bulk}} - 1]/\alpha_i \equiv (I_{\mathrm{norm}} - 1)/\alpha_i$ as a function of α_i [Fig. 1(c)] yielding $\Gamma_i/c_{i\infty}$. Quantitatively, we obtain $(\Gamma/c_\infty)_{\mathrm{Cl}^-} = -3.54 \pm 0.16$ Å and $(\Gamma/c_\infty)_{\mathrm{K}^+} = -3.69 \pm 0.14$ Å for KCl solution. The fit provided a zero slope in agreement with the extremely small surface potential of KCl [related to the second term in Eq. (1)]. Incorporating these values into Gibbs equation, yielded $d\gamma/dc = 1.77$ (mN/m)/(mol/L) which is in good agreement with the surface tension measurements. This corresponds to a negative surface excess of $\approx -2.2 \times 10^{17}$ ions/m^2 which is equivalent to 1 ion lacking per 4.5 nm^2 or 30 nm^3. As reliable data could be obtained with 0.01 M solutions, the resolution of the experiment is at least 1 ion in 300 nm^3.

The very small difference, if any, which we obtain between the K^+ and Cl^- adsorptions is clearly related to electroneutrality as the penetration depth is larger than the Debye length (9.6 Å) in this experiment. We envisaged a strategy to overcome this constraint and enhance the sensitivity to very short-range interfacial interactions by turning towards mixtures. Indeed, in a mixture of, for example, KCl and KI, electroneutrality can be achieved either by Cl^- or by I^-, and the short-range interactions are brought into play more effectively which can influence the interfacial equilibria significantly. The resulting outcome is shown in Fig. 1(d) where it is evident that I^- is attracted more to the interface than Cl^-, K^+ ensuring electroneutrality. This is, to our knowledge, the first direct evidence of the larger propensity of I^- compared to Cl^- at the interface of liquid aqueous electrolytes under ambient conditions. The surface compositions of different alkali-halide solutions and mixtures are given in Table I.

The accuracy of these data proved to be good enough to allow for a detailed analysis in terms of ion-surface interaction potential. In the absence of a first-principles theory to predict the surface properties and to capture the specific interactions, we extend the approach of Ref. [15]. In a first step, the ion-ion correlations in the bulk electrolyte are calculated with the Ornstein-Zernike equation and the HNC closure for the required ionic densities. The radii and polarizabilities take the adjusted values of Ref. [15] which reproduce the thermodynamical properties of the electrolyte up to a few molar. In a second step, the electrolyte is put in contact with a single big sphere (extra component at infinite dilution). As long as the radius R of this sphere is large compared to the characteristic distances in the electrolyte, its precise value is irrelevant and the sphere-electrolyte interface mimics a flat air-water interface. $R = 50$ Å is sufficient in practice. The HNC equation is solved for the pair distribution functions between the big sphere and the ions and gives the local ionic profiles $c_i(z) = c_{i\infty} g_i(z)$. The interface-ion pair potential $u_i(z)$ contains the hard-sphere contribution, the *generic* screened image force contribution, the dispersion contribution, and an extra *specific*, adjustable, short-range potential, needed to quantitatively understand the experimental data, $u_i^{\mathrm{extra}} = K_i \exp(-z/d)$ (exact shape is not important) with fixed range $d = 1$ Å and adjustable strength K_i. As cations, except H^+, are known to have a smaller effect on the surface tension, we decided to use a nonzero u_i^{extra} for anions and H^+ only. Using a strength of the effective potential of $-4.0 k_B T$ at contact for Cl^-, $-4.7 k_B T$ for Br^-, $-4.4 k_B T$ for I^-, and $-3.15 k_B T$ for H^+, excellent agreement is obtained with the measured Γ_i values (Table I), except for lithium salts, possibly indicating that a slightly repulsive short-range potential is needed for this cation. It is quite remarkable that we are able to reproduce about 20 independent measurements with only 4 adjustable parameters, supporting the idea that specific effects are indeed short-range couplings. In this respect, it is interesting to note that this simple model gives a quantitative description of the concentration dependence of the surface excess. In the case of HCl, we are able to reproduce even the sign reversal of the surface excess which is slightly negative for 0.1 M and positive with higher screening at 1 M concentration. Further, our work emphasizes the fact that the surface equilibria mainly result from a subtle balance between the dispersion interaction u^{disp} and the short-range potential u^{extra}, while the image charge force u^{image} plays a less significant role [Fig. 2(a)]. In the case of Cl^- and I^-, for example, the dispersion forces are almost

TABLE I. Measured and calculated surface excess (Γ/c) for different alkali-halide solutions. For Na in 0.1 M NaCl + NaI, Γ_{calc}/c is -2.98 Å/(mol/L).

	NaCl	NaCl	HCl	HCl	KCl		LiCl	NaCl + NaI		KCl + KI			CsCl + CsI			LiCl + LiBr	
c (mol/L)	0.01	0.1	0.1	1.0	0.1		1.0	0.1		0.1			0.1			0.1	
	Cl^-	Cl^-	Cl^-	Cl^-	Cl^-	K^+	Cl^-	Cl^-	I^-	Cl^-	I^-	K^+	Cl^-	I^-	Cs^+	Cl^-	Br^-
Γ_{meas} (Å)	−6.3	−4.02	−0.5	+.55	−3.54	−3.69	−3.35	−4.95	−1.90	−4.05	−2.00	−3.10	−4.30	−1.90	−3.10	−4.25	−2.60
	±1.5	±0.15	±0.2	±0.15	±0.16	±0.13	±0.1	±0.3	±0.15	±0.15	±0.1	±0.1	±0.1	±0.1	±0.1	±0.35	±0.15
Γ_{calc}	−6.0	−3.8	−0.51	+0.56	−3.65	−3.65	−2.85	−3.83	−2.12	−3.72	−1.99	−2.85	−3.69	−2.02	−2.85	−3.22	−2.56

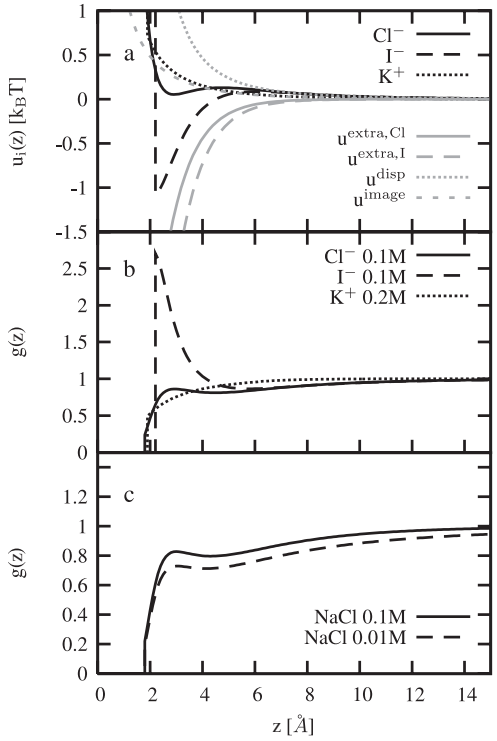

FIG. 2. Interface-ion pair potential $u_i(z)$ and concentration profiles $g(z)$ of ions obtained by fitting the effective strength of the short-range exponential potential as described in the text. (a) Interface-ion potential for Cl^-, I^-, and K^+ in KCl 0.1 M + KI 0.1 M mixture (black lines). The gray dotted line represents the dispersion interaction for Cl^- u^{disp}, almost equal to that for I^-. The gray short-dashed line represents the image charge potential u^{image} which is the same for all ions. The solid gray lines and long-dashed gray lines represent the additional short-range exponential potential u^{extra} for Cl^- and I^-, respectively. (b) Concentration profiles in KCl 0.1 M + KI 0.1 M mixture. (c) Cl^- concentration profile in NaCl 0.1 M and NaCl 0.01 M.

equal, and the difference in the top 5 Å is mainly due to u^{extra}. The effective potential values *at contact* for Cl^- and I^- being close to each other, the potential is more attractive for the biggest I^- ion. However, the minimum in the potential is reduced by a factor of 4 due to the dispersion interaction. More generally, as the ionic radii range as $Cl^-(1.81\ \text{Å}) < Br^-(1.96\ \text{Å}) < I^-(2.2\ \text{Å})$, we recover the Hofmeister series $\Gamma(I^-) > \Gamma(Br^-) > \Gamma(Cl^-)$.

Knowing the effective short-range potential, the interfacial distribution of ions can be calculated. Figure 2 shows the result of such calculation for NaCl at two different concentrations and for the mixture of KCl and KI. As expected, the main effect of an increase in salt concentration is to reduce the repulsion of the image charge, and beyond that to wash out the profile. In the mixture, I^- is more strongly attracted to the surface than Cl^-. Interestingly, these profiles are in excellent agreement with the numerical simulations [16] for Cl^- and I^-.

J. D. and V. P. acknowledge support of the Indo-French center for the promotion of advanced research. Support from ANR under Grant No. ANR-06-BLAN-0276 is gratefully acknowledged. The authors benefitted from discussions with O. Spalla who pointed out the interest of competitive adsorption experiments.

*Present address: Max Planck Institute of Colloids and Interfaces, Wissenschaftspark Golm, D-14424 Potsdam, Germany.
†jean.daillant@cea.fr

[1] K. D. Collins and M. W. Washabaugh, Q. Rev. Biophys. **18**, 323 (1985).
[2] M. G. Cacace, E. M. Landau, and J. J. Ramsden, Q. Rev. Biophys. **30**, 241 (1997).
[3] F. Hofmeister, Arch. Exp. Pathol. Pharmakol. **24**, 247 (1888).
[4] D. L. Hall and P. L. Darke, J. Biol. Chem. **270**, 22697 (1995).
[5] A. I. Bush, W. H. Pettingell, G. Multhaup, M. D. Paradis, J. P. Vonsattel, J. F. Gusella, K. Beyreuther, C. L. Masters, and R. E. Tanzi, Science **265**, 1464 (1994).
[6] L. K. Koopal, T. Saito, J. P. Pinheiroa, and W. H. van Riemsdijk, Colloids Surf. A **265**, 40 (2005).
[7] K. W. Oum, M. J. Lakin, D. O. DeHaan, T. Brauers, and B. J. Finlayson-Pitts, Science **279**, 74 (1998).
[8] K. L. Foster, R. A. Plastridge, J. W. Bottenheim, P. B. Shepson, B. J. Finlayson-Pitts, and C. W. Spicer, Science **291**, 471 (2001).
[9] P. K. Weissenborn and R. J. Pugh, J. Colloid Interface Sci. **184**, 550 (1996).
[10] L. Onsager and N. N. T Samaras, J. Chem. Phys. **2**, 528 (1934).
[11] Y. Levin and J. E. Flores-Mena, Europhys. Lett. **56**, 187 (2001).
[12] E. Ruckenstein and M. Manciu, Adv. Colloid Interface Sci. **105**, 177 (2003).
[13] S. A. Edwards and D. R. M. Williams, Europhys. Lett. **74**, 854 (2006).
[14] B. W. Ninham and V. Yaminsky, Langmuir **13**, 2097 (1997).
[15] W. Kunz, L. Belloni, O. Bernard, and B. W. Ninham, J. Phys. Chem. B **108**, 2398 (2004).
[16] P. Jungwirth and D. Tobias, J. Phys. Chem. B **105**, 10 468 (2001).
[17] P. Jungwirth and D. J. Tobias, Chem. Rev. **106**, 1259 (2006).
[18] D. Liu, G. Ma, L. M. Levering, and H. C. Allen, J. Phys. Chem. B **108**, 2252 (2004).
[19] E. A. Raymond and G. L. Richmond, J. Phys. Chem. B **108**, 5051 (2004).
[20] R. Weber, B. Winter, P. M. Schmidt, W. Widdra, I. V. Hertel, M. Dittmar, and M. Faubel, J. Phys. Chem. B **108**, 4729 (2004).
[21] S. Ghosal, J. C. Hemminger, H. Bluhm, B. S. Mun, E. L. D. Hebenstreit, G. Ketteler, D. F. Ogletree, F. G. Requejo, and M. Salmeron, Science **307**, 563 (2005).
[22] E. Sloutskin, J. Baumert, B. M. Ocko, I. Kuzmenko, A. Checco, L. Tamam, T. Ofer, E. Gog, O. Gang, and M. Deutsch, J. Chem. Phys. **126**, 054704 (2007).
[23] M. van Gysel, P. Lemberge, and P. van Espen, X-Ray Spectrom. **32**, 434 (2003).